



Development and Characterization of 3D Printable Thermite Component Materials

Matthew M. Durban, Alexandra M. Golobic, Eric V. Bukovsky, Alexander E. Gash, and Kyle T. Sullivan*

Additive manufacturing (AM) has recently shown great promise as a means to tailor a wide range of material properties, both quasi-static and dynamic. An example of controlling the dynamic behavior is to tailor the chemical energy release rate in composite energetic materials such as thermites – which are a subset of pyrotechnics that use a metal fuel and a metal oxide as an oxidizer. Since these materials are most hazardous once finely mixed, the approach taken here is to formulate the fuel and oxidizer separately such that they can be mixed on-the-fly. Herein, the development, formulation, and characterization of two respective aqueous 3D printable inks consisting of Al and CuO are discussed. The rheological properties and ability of the material to span gaps are characterized. To demonstrate that the materials could be mixed and sustain a reaction, the inks are fed into a static mixing nozzle and extruded into a high-aspect ratio test strip. Upon drying, the material can be ignited and sustain a propagation through the part. These results present a facile, and safe, way to AM thermite which can be used for more detailed follow on studies looking at the role of architecture on the reactivity.

The field of 3D printing has recently experienced a massive surge in growth and maturation, especially with regard to the development of thermoplastics,^[1] UV curables,^[2] silicones,^[3] and a variety of metal powder-based materials.^[4] The ability to additively fabricate structures with novel architectures and render materials with enhanced properties has been demonstrated and well established.^[5] This has been applied to control mechanical,^[6–10] optical,^[11–13] and electronic^[14–16] properties of materials, as well as enable new functional materials.^[17–20]

While a large portion of studies focus on quasi-static applications, additive manufacturing (AM) has also shown promise as a means to tailor dynamic properties, such as the rate of chemical energy release in reactive materials (RMs).^[21–25] RMs are a subset of energetic materials and are composites that, upon ignition, give rise to the rapid liberation of energy in the form of heat and/or pressure. Further within the subset of RMs, materials can be defined as either intermetallics (metal/metal) or thermites (metal/metal oxide). In a recent paper, it was

shown that architecture could be used to manipulate the reactivity of aluminum/copper oxide (Al/CuO) thermites by tailoring the flow of gases and entrained particles using structure.^[23] A similar behavior had previously been seen in porous-Si-based energetic materials.^[21] This is an exciting result in that it enables one to tailor the energy release rate in such materials without defaulting to the conventional approach of changing the formulation.

To further expand upon the previous results, we seek to develop AM formulations which can enable a wide range of architectures to be printed. With this, we can design test articles to further understand and quantify to what extent architecture can be used to control reactivity. However, the direct printing of thermite raises safety concerns since, as-mixed, the materials can lead to a rapid reaction in the event of accidental ignition. A far safer approach would be to formulate the

precursor materials separately, and then to directly mix during the printing process.

In this work, we formulated an Al and a CuO precursor ink separately. One factor in the choice of these precursors was to pick two systems that could be formulated with similar rheological properties, as disparate rheological properties could lead to potential issues during mixing operations. Al and CuO powder feedstock materials were formulated using micron-sized particles of the materials incorporated into an aqueous hydrogel matrix to render an extrudable prethermite “ink.” The rheology of these high solids loaded prethermite inks had to be such that the inks could be extruded through a nozzle (i.e., shear thinning) as wet filaments. The formulation parameters can be seen in **Table 1**, and some considerations are discussed later in the text. Once formulated, the inks were loaded into a syringe and mounted on the printer. A schematic of the printing setup is shown in **Figure 1**. The basic components of this setup are highlighted, and include two mounts for syringes, linear extrusion motors, and a precise xyz positioning stage (Aerotech). After extrusion, parts are dried in air and the as-deposited printed filaments retain the properties possessed by the dry powder feedstock material. The formulation and printability of the individual materials are investigated; we subsequently show that the two materials can be mixed on-the-fly to render an ignitable thermite ink.

Dr. M. M. Durban, A. M. Golobic, Dr. E. V. Bukovsky, Dr. A. E. Gash, Dr. K. T. Sullivan
Lawrence Livermore National Laboratory
Livermore, CA 94550, USA
E-mail: sullivan34@llnl.gov

DOI: 10.1002/admt.201800120

Table 1. 3D printable aqueous Al and CuO ink formulation details.

Component	Al [wt. %]	CuO [wt. %]
5% Methocel F4M	23%	13%
Neutral Darvan 821A/PEI ^{a)}	2%	2%
Al powder (H-2 grade) ^{b)}	75%	–
CuO powder (10 μm grade) ^{b)}	–	85%

^{a)}50/50 blend of Darvan 821A surfactant and polyethyleneimine (PEI) neutralized through the dropwise addition of concentrated HCl and monitored with a Thermo Scientific Orion 4-Star Plus Portable pH/Conductivity Meter; ^{b)}Al and CuO loading effectively equivalent to 52 and 47 vol%, respectively.

With regard to preparing the aqueous Al and CuO prethermite inks, we based our formulations off of a recipe similar to that done by Rao et al.^[26] to develop a 3D printable aqueous colloidal–gel matrix, suitable for loading with ceramic or various other solid powder materials. This report served as an effective starting point for the development of our prethermite ink components, but some modifications were necessary. As described, the aqueous ink matrix was composed of a methylcellulose hydrogel, which was reinforced through the formation of an ionic-bridging network between the carboxylic acid groups of a poly(acrylic acid) and the amine groups of a polyethyleneimine component. A key feature of this system can be attributed to its rheological stability and the avoidance of formed solid precipitates.

However, one aspect of the formulation must be accounted for prior to loading the matrix with potentially reactive metal filler materials. The combined addition of poly(acrylic acid) (Darvan 821A) and polyethyleneimine can result in the generation of ammonia and ammonium hydroxide species, rendering a strongly basic ink matrix that can strip the passivating aluminum oxide layer and begin degrading the reactive filler, resulting in the persistent generation of hydrogen gas. This gas generation led to poor 3D printing performance and behavior due to the extrusion of porous filaments and an unacceptable buildup of capacitance within the syringe ink reservoir

(see **Figure 2**). To overcome these issues, the poly(acrylic acid) and polyethyleneimine components were combined and neutralized with concentrated HCl prior to being added to the hydrogel matrix. pH neutralization of the ink matrix served to stabilize the ink within the syringe and remedy the gas generation and 3D printing inconsistencies associated with a strongly basic ink matrix; a strong ammonia smell released by the ink itself was also eliminated due to formation of odorless ammonium chloride.

With regard to determining the appropriate loading rate for the Al and CuO reactive metal filler powders, ink formulations were iteratively prepared by progressively increasing their respective loading rates until reaching a balanced level that was not exceedingly difficult to extrude and print and not too quick to dry out. Maximizing the solids is an important parameter in energetic materials, as it pertains to volumetric energy density. In this case, an Al loading of 74 wt% (52 vol%) was achieved for the Al ink and a CuO loading of 85 wt% (47 vol%) was achieved for the CuO ink. The Al and CuO particle sizes nominally dictated the experimentally determined filler loading rates due to surface area related particle–matrix wetting effects. The manufacturer reported particle size distribution for the Al powder (Valimet H-2 spherical) was <7.5 μm (50% < 3.5 μm) and <10 μm for the CuO powder (Sigma-Aldrich).

In order to assess the printability of the Al and CuO prethermite inks, yield stress measurements were performed via oscillatory rheology. A plot of the modulus ratio (G'/G'') versus oscillatory stress revealed a yield stress value of ≈65 Pa for the Al ink and ≈20 Pa for the CuO ink (yield stress was defined as the oscillatory stress corresponding to 90% of the storage modulus plateau, see **Figure 3A,B**). An allometric model was fit to the shear rate versus shear stress plot, revealing that both the Al and CuO prethermite inks exhibited pseudoplastic behavior (flow behavior index, $n < 1$) based on the Ostwald–de Waele power law describing non-Newtonian fluids (see **Figure S1**, Supporting Information). The spanning performance of the prethermite inks was also experimentally confirmed and verified

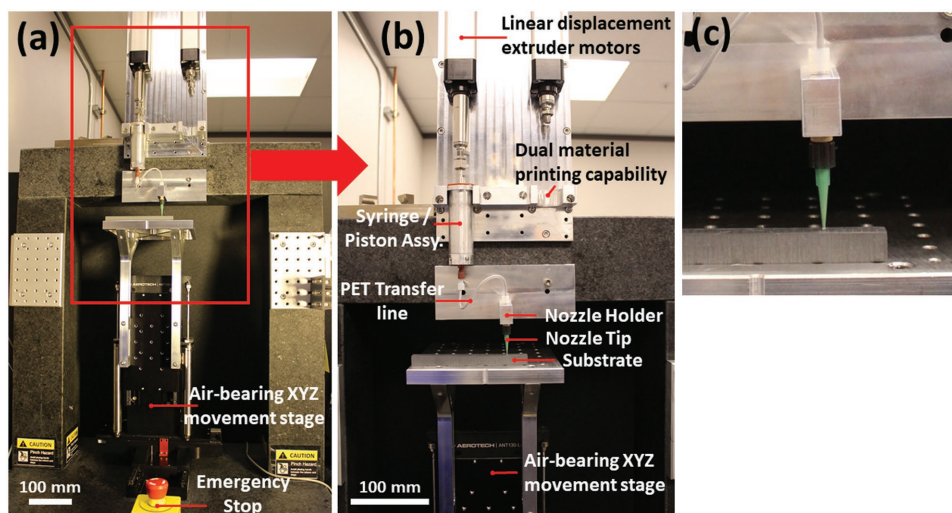


Figure 1. The custom Aerotech 3D printer showing a) an overview of the gantry and movement stage and b) a more detailed view of the extrusion assembly, printing stage, and c) the nozzle where material is extruded through.

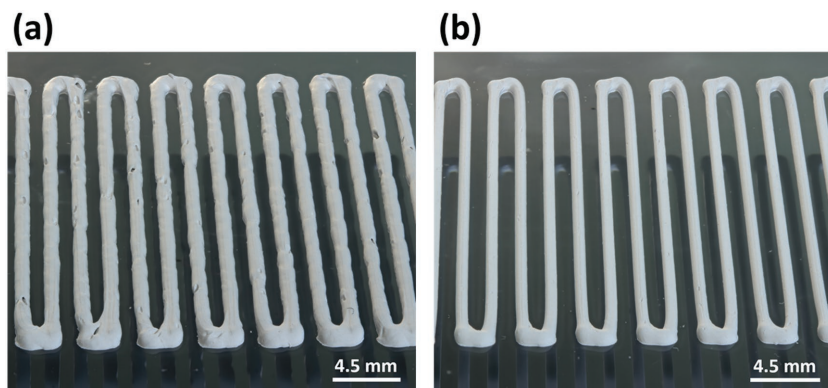


Figure 2. 3D printed serpentine patterns printed from a) an untreated aqueous Al prethermite ink and b) a treated (neutralized) aqueous Al prethermite ink.

through the printing of the Al and CuO inks onto 120×40 mm rectangular substrates with a V-shaped cut taken out of one end of the substrate. The dimensions of the V-shaped cut were 85 mm long, encompassing a 7.2° angle, with a maximal spanning distance of 10 mm at the terminal edge of the cut. A serpentine pattern (1 mm filament spacing) was printed in such a way that the extruded filaments ($580 \mu\text{m}$ nozzle) perpendicularly spanned the V-shaped cut, progressively spanning the substrate gap until reaching a peak gap distance of 10 mm. It is not common to build large, unsupported spanning structures in parts, however, this ability simply serves to demonstrate the exceptional printability of the materials. In fact, the Al and CuO inks demonstrated the ability to span the entire length of

the engineered gap to 10 mm with minimal sagging, see Figure 3C,D.

Another aspect of 3D printing aqueous RMs that should be accounted for is the substrate material used for printing. To ensure the safety and performance of the printed RMs, the selected printing substrate should be entirely inert to the components within the printed inks. For example, while particular metallic substrates such as Al and steel may be robust to the thermite combustion process, these substrates were shown to not be entirely inert to the aqueous prethermite inks. Undesirable interactivity or degradation of the substrate surface can limit and inhibit adhesion of the printed ink filaments after drying. Therefore, chemically inert

substrate materials such as ceramics (alumina, zirconia, etc.) should be employed instead. Sample images of dried printed filaments of Al and CuO on Al, steel, and alumina can be seen in **Figure 4**, demonstrating the undesired oxidation and reactivity of the aqueous prethermite inks with various substrate materials.

To demonstrate the reactivity of the formulated 3D printable aqueous prethermite inks, the Al and CuO inks were fed into a Nordson EFD disposable static mixer at an equivalence ratio of 1.0 (i.e., a molar ratio of Al:CuO of 2:3 to completely oxidize the Al to Al_2O_3). The static mixing nozzle had 24 elements; this length was simply chosen such that the ink appeared visually homogeneous upon extrusion. Evaluating

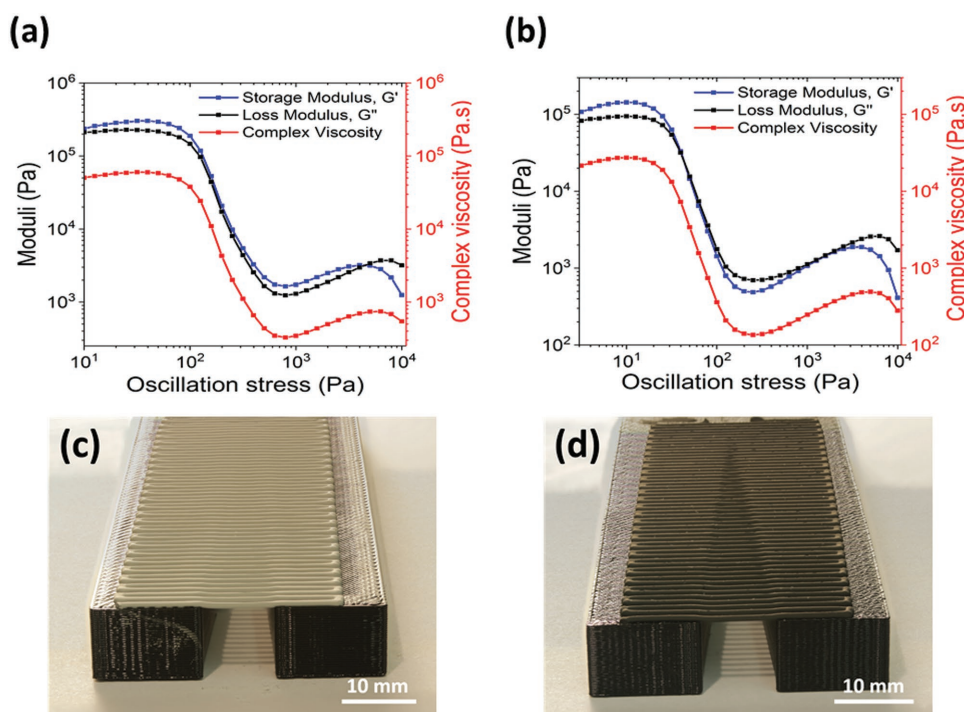


Figure 3. Oscillatory rheology showing modulus and viscosity curves for the a) aqueous Al prethermite ink and b) aqueous CuO prethermite ink. Images demonstrating spanning capabilities through 3D printed bridging serpentine patterns over a peak spanning gap of 10 mm for the c) aqueous Al prethermite ink and d) aqueous CuO prethermite ink.

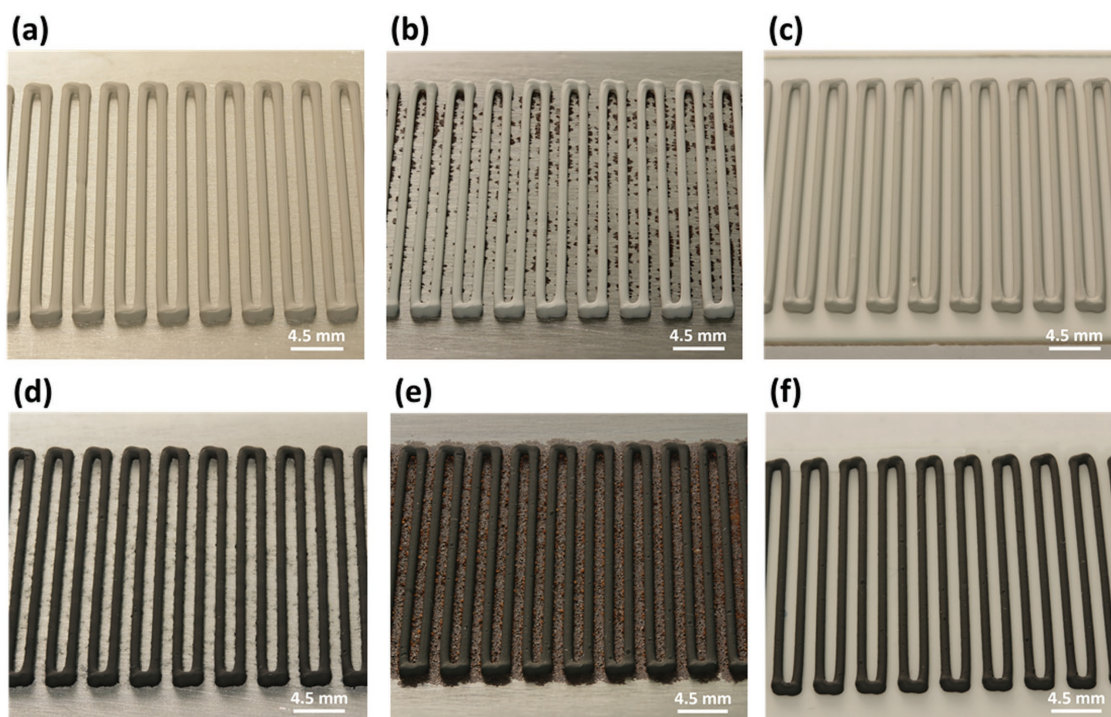


Figure 4. Serpentine patterns of the aqueous Al prethermite ink 3D printed onto various substrate materials, including a) Al, b) spring steel, and c) alumina ceramic. Corresponding serpentine patterns of the aqueous CuO prethermite ink 3D printed onto d) Al, e) spring steel, and f) alumina ceramic.

the requirements to achieve complete mixing is a topic which will be investigated in a later study. The Al and CuO inks were passed through the static mixing nozzle and through a 0.58 mm (20 gauge) tapered conical tip to create a ≈ 10 cm long strip. A ceramic substrate was used for this, given the substrate effects discussed earlier (see Figure 4). After printing, the test article was allowed to dry overnight under ambient conditions. While the thermite ink was comprised of approximately 80% reactive metal/metal oxide powder within an aqueous matrix, upon the elimination of water from the thermite ink due to drying, the printed thermite filaments were noted to consist of $\approx 97\%$ reactive thermite. The remaining 3% could be attributed to dry methylcellulose, poly(acrylic acid), and polyethyleneimine. The methylcellulose network within the dry printed filaments served to effectively bind together what would otherwise comprise dry thermite powder and rendered the dry filaments as being quite robust and resistant to cracking due to water-loss-induced shrinkage.

The dry printed thermite filaments were ignited with a butane torch and a self-propagating flame could be observed. This event was recorded using a Phantom Miro M110 high-speed camera at 1000 fps. A photograph of the printed mixed thermite and propagating thermite flame front can be seen in **Figure 5**. The flame front position versus time from the high-speed movie was recorded, and it can be seen that the propagation occurs with a speed of approximately 12 cm s^{-1} . While reporting flame speed is common in the literature, the absolute value on its own is not all that meaningful other than to roughly compare with other formulations. Both the formulation and configuration are well known to affect this value, and this must be considered when making such comparisons. Future work will look at the efficacy

of mixing, as well as to investigate and quantify how printed features can be used to *control* this flame speed. However, the current work is a necessary precursor towards doing these more elaborate combustion studies.

In summary, we have demonstrated the successful formulation, printing, and combustion of aqueous prethermite inks based on an Al and CuO reactive thermite system. Aqueous-based inks were formulated, and their rheological properties and printability examined. These inks were then mixed in situ using a static mixer to render a printed thermite test article, and the article was shown to sustain a propagating flame. This work gives a facile, and safe, route to do more detailed studies to elucidate the effects of mixing and architecture on the energy release rate in thermites.

Experimental Section

Preliminary ink formulations were based on prior formulation work reported by Rao et al.^[9] However, modifications to the ink formulation had to be made. Specifically, it was found early on that the unmodified formulations exhibited a degree of basicity that led to the progressive decomposition of Al. The formulation thus required acid neutralization to yield a stable printable ink material, the details of which are described in the current section as follows. Aluminum sheet (1/8 in.), hardened spring steel (1/16 in.), aluminum oxide ceramic sheet (1/8 in.), and alumina-silicate ceramic bar stock (1/2 in.) substrates were obtained from McMaster-Carr and were machine cut to appropriate widths as necessary for printing.

Preparation of the 5% Methylcellulose Hydrogel Matrix: Manufacturer procedures written for Methocel F4M (Dow) using a hot/cold solution

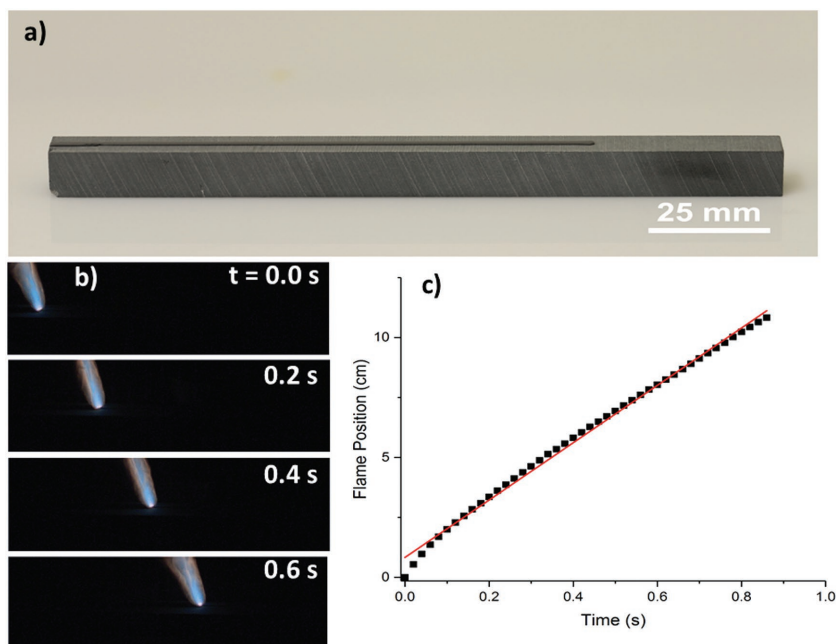


Figure 5. a) Printed mixed thermite on a ceramic block substrate. b) A series of snapshots taken ≈ 200 ms apart during the flame propagation. c) The position of the flame front versus time. The slope can be used to report the propagation speed.

preparation technique were followed for a 5% Methocel F4M batch (100 g). A beaker was charged with Methocel F4M (5 g), which was thoroughly mixed with hot water (35 g) at 90 °C. The mixture was agitated and mixed until all the Methocel particles were wetted and a consistent dispersion was obtained. The remaining water (60 g) was added as cold water while mixing and agitating the suspension, yielding a highly viscous material. The mixture was agitated until obtaining a smooth solution. The solution was slowly cooled to room temperature while agitating and mixing for at least 20 min, yielding a clear thick material that was deeply aerated with bubbles. Allowing the material to rest overnight yielded a clear homogeneous bubble-free hydrogel material.

Preparation of the Aqueous Al and CuO Inks: A Flacktek Max 100 mixing cup was charged with the 5% Methocel F4M hydrogel (6.90 g [Al] or 7.80 g [CuO]) and an acid-neutralized 50/50 blend of Darvan 821A surfactant and polyethyleneimine (0.60 g [Al] or 1.20 g [CuO]). Al powder (22.5 g, 3.5 μm H-2 grade, Valimet, Inc.) or CuO powder (51.0 g, 10 μm grade, Sigma-Aldrich) was added to the mixing cup with a spatula. The components were speedmixed (Flacktek DAC 150.1 FVZ-K) at 3500 rpm for 15 s. The sides, bottom, and bottom corners or edges of the mixing cup were scraped with a spatula and the Al or CuO ink blend was speedmixed again at 3500 rpm for 15 s. The blended ink was scraped and speedmixed for an additional cycle if deemed necessary based on the consistency and uniformity of the prepared paste. Note that Al particles can exothermically react with water; thus, one should exercise extreme caution when mixing inks in a high-shear setup such as a Flacktek SpeedMixer. Accidental reactions with water can lead to pressure buildup within the mixing cup; however, one can mitigate this by minimizing the mass of Al or the mixing time and also allowing a sufficient cooling duration between cycles. After mixing, the paste was quickly transferred to a Nordson EFD syringe barrel (with a covered tip) to prevent water loss due to drying under air exposure. The syringe was placed in a 30 cc syringe holder and mixed with the Flacktek SpeedMixer at 3500 rpm for 15 s. An appropriate piston was inserted into the rear of the syringe barrel to eliminate any trapped air and prepare the syringe for printing.

3D Printing of P: All reagents and materials were obtained from their respective manufacturer as listed above and were used as-is

without further purification. Formulations were prepared using a Flacktek DAC 150.1 FVZ-K SpeedMixer for compounding. Yield stress and viscosity measurements were obtained with a TA Instruments AR2000EX rheometer equipped with a stainless steel 40 mm Peltier parallel plate under a 1 mm sample gap spacing. Corresponding aqueous Al and CuO prethermite ink filled syringes were each attached to a linear-displacement motor, which supplied the appropriate displacement to feed the ink into a Nordson EFD conical syringe tip attached via Luer Lock. The extruder assembly was subsequently affixed to the static gantry of a custom Aerotech air-bearing xyz open frame movement stage, which was controlled via an A3200 controller through an Aerotech A3200 CNC operator interface (v5.05.000). G-code instructions were programmed and run through the controller software to generate component ink filament structures in both linear and serpentine (spanning) patterns. Figure 1 shows images of the experimental 3D printing system used to create all the parts and structures presented in this report. The inks were printed at a rate of 15 mm s⁻¹ onto flat Al, spring steel, alumina, and ceramic substrates to study the effects of substrate–ink interactions and onto a 3D printed ABS substrate to assess the spanning capabilities of each respective aqueous prethermite ink.

Supporting Information

Supporting Information is available from the Wiley Online Library or from the author.

Acknowledgements

This work was performed under the auspices of the U.S. Department of Energy by Lawrence Livermore National Laboratory under Contract DE-AC52-07NA27344. Funding provided by LDRD16-ERD-040. IM release LLNL-JRNL-748707.

Conflict of Interest

The authors declare no conflict of interest.

Keywords

3D printing, additive manufacturing, reactive materials, thermite

Received: April 15, 2018

Revised: October 1, 2018

Published online:

- [1] a) M. G. M. Marascio, J. Antons, D. P. Pioletti, P.-E. Bourban, *Adv. Mater. Technol.* **2017**, *2*, 1700145; b) G. Ellson, X. Carrier, J. Walton, S. F. Mahmood, K. Yang, J. Salazar, W. E. Voit, *J. Appl. Polym. Sci.* **2018**, *135*, 45574.
[2] a) A. Selimis, V. Mironov, M. Farsari, *Microelectron. Eng.* **2015**, *132*, 83; b) M. Zarek, M. Layani, I. Cooperstein, E. Sacyani, D. Cohn, S. Magdassi, *Adv. Mater.* **2016**, *28*, 4449.

- [3] M. M. Durban, J. M. Lenhardt, A. S. Wu, W. Small, T. M. Bryson, L. Perez-Perez, D. T. Nguyen, S. Gammon, J. E. Smay, E. B. Duoss, J. P. Lewicki, T. S. Wilson, *Macromol. Rapid Commun.* **2017**, *39*, 1700563.
- [4] a) W. J. Sames, F. A. List, S. Pannala, R. R. Dehoff, S. S. Babu, *Int. Mater. Rev.* **2016**, *61*, 315; b) W. E. Frazier, *J. Mater. Eng. Perform.* **2014**, *23*, 1917.
- [5] a) F. Momeni, S. M. Mehdi Hassani N, X. Liu, J. Ni, *Mater. Des.* **2017**, *122*, 42; b) A. S. Wu, W. Small Iv, T. M. Bryson, E. Cheng, T. R. Metz, S. E. Schulze, E. B. Duoss, T. S. Wilson, *Sci. Rep.* **2017**, *7*, 4664.
- [6] C. Schumacher, B. Bickel, J. Rys, S. Marschner, C. Daraio, M. Gross, *ACM Trans. Graphics* **2015**, *34*, 136:1.
- [7] X. Zheng, W. Smith, J. Jackson, B. Moran, H. Cui, D. Chen, J. Ye, N. Fang, N. Rodriguez, T. Weisgraber, C. M. Spadaccini, *Nat. Mater.* **2016**, *15*, 1100.
- [8] E. B. Duoss, T. H. Weisgraber, K. Hearon, C. Zhu, W. Small, T. R. Metz, J. J. Vericella, H. D. Barth, J. D. Kuntz, R. S. Maxwell, C. M. Spadaccini, T. S. Wilson, *Adv. Funct. Mater.* **2014**, *24*, 4905.
- [9] X. Zheng, H. Lee, T. H. Weisgraber, M. Shusteff, J. DeOtte, E. B. Duoss, J. D. Kuntz, M. M. Biener, Q. Ge, J. A. Jackson, S. O. Kucheyev, N. X. Fang, C. M. Spadaccini, *Science* **2014**, *344*, 1373.
- [10] Y. Chen, T. Li, Z. Jia, F. Scarpa, C. Yao, L. Wang, *Mater. Des.* **2018**, *137*, 226.
- [11] D. J. Lorang, D. Tanaka, C. M. Spadaccini, K. A. Rose, N. J. Cherepy, J. A. Lewis, *Adv. Mater.* **2011**, *23*, 5055.
- [12] I. K. Jones, Z. M. Seeley, N. J. Cherepy, E. B. Duoss, S. A. Payne, *Opt. Mater.* **2018**, *75*, 19.
- [13] D. T. Nguyen, C. Meyers, T. D. Yee, N. A. Dudukovic, J. F. Destino, C. Zhu, E. B. Duoss, T. F. Baumann, T. Suratwala, J. E. Smay, R. Dylla-Spears, *Adv. Mater.* **2017**, *29*, 1701181.
- [14] Z. Qi, J. Ye, W. Chen, J. Biener, E. B. Duoss, C. M. Spadaccini, M. A. Worsley, C. Zhu, *Adv. Mater. Technol.* **2018**, *3*, 1870026.
- [15] J. J. Adams, E. B. Duoss, T. F. Malkowski, M. J. Motala, B. Y. Ahn, R. G. Nuzzo, J. T. Bernhard, J. A. Lewis, *Adv. Mater.* **2011**, *23*, 1335.
- [16] C. Zhu, T. Y.-J. Han, E. B. Duoss, A. M. Golobic, J. D. Kuntz, C. M. Spadaccini, M. A. Worsley, *Nat. Commun.* **2015**, *6*, 6962.
- [17] S. Babaei, J. Shim, J. C. Weaver, E. R. Chen, N. Patel, K. Bertoldi, *Adv. Mater.* **2013**, *25*, 5044.
- [18] A. Maiti, W. Small, J. P. Lewicki, T. H. Weisgraber, E. B. Duoss, S. C. Chinn, M. A. Pearson, C. M. Spadaccini, R. S. Maxwell, T. S. Wilson, *Sci. Rep.* **2016**, *6*, 24871.
- [19] J. A. Lewis, *Adv. Funct. Mater.* **2006**, *16*, 2193.
- [20] Y. Chen, T. Li, F. Scarpa, L. Wang, *Phys. Rev. Appl.* **2017**, *7*, 024012.
- [21] a) V. S. Parimi, S. Huang, X. Zheng, *Proc. Combust. Inst.* **2017**, *36*, 2317; b) V. S. Parimi, A. Bermúdez Lozda, S. A. Tadigadapa, R. A. Yetter, *Combust. Flame* **2014**, *161*, 2991.
- [22] B. Clark, J. McCollum, M. Pantoya, R. Heaps, M. Daniels, *AIP Adv.* **2015**, *5*, 087128.
- [23] K. T. Sullivan, C. Zhu, E. B. Duoss, A. E. Gash, D. B. Kolesky, J. D. Kuntz, J. A. Lewis, C. M. Spadaccini, *Adv. Mater.* **2016**, *28*, 1934.
- [24] F. Ruz-Nuglo, L. Groven, *Adv. Eng. Mater.* **2018**, *20*, 1700390.
- [25] A. Murray, T. Isik, V. Ortalan, I. Gunduz, S. Son, G. Chiu, J. Rhoads, *J. Appl. Phys.* **2017**, *122*, 184901.
- [26] R. B. Rao, K. L. Krafcik, A. M. Morales, J. A. Lewis, *Adv. Mater.* **2005**, *17*, 289.